Supplyment

Observations of the vertical distributions of summertime atmospheric pollutants in Nam Co: OH production and source analysis

Chengzhi Xing[1], Cheng Liu[2,1,3,5,*], Chunxiang Ye[4,*], Xiangguang Ji[7], Jingkai Xue[6], Jinping Ou[1], Hongyu Wu[6], and Qihou Hu[1]

[1] Key Lab of Environmental Optics & Technology, Anhui Institute of Optics and Fine Mechanics, Hefei Institutes of Physical Science, Chinese Academy of Sciences, Hefei, 230031, China
[2] Department of Precision Machinery and Precision Instrumentation, University of Science and Technology of China, Hefei, 230026, China
[3] Center for Excellence in Regional Atmospheric Environment, Institute of Urban Environment, Chinese Academy of Sciences, Xiamen, 361021, China
[4] College of Environmental Sciences and Engineering, Peking University, 100871 Beijing
[5] Key Laboratory of Precision Scientific Instrumentation of Anhui Higher Education Institutes, University of Science and Technology of China, Hefei, 230026, China
[6] School of Environmental Science and Optoelectronic Technology, University of Science and Technology of China, Hefei, 230026, China
[7] Institute of Physical Science and Information Technology, Anhui University, Hefei, 230601, China

*Corresponding author. E-mail: chliu81@ustc.edu.cn; c.ye@pku.edu.cn

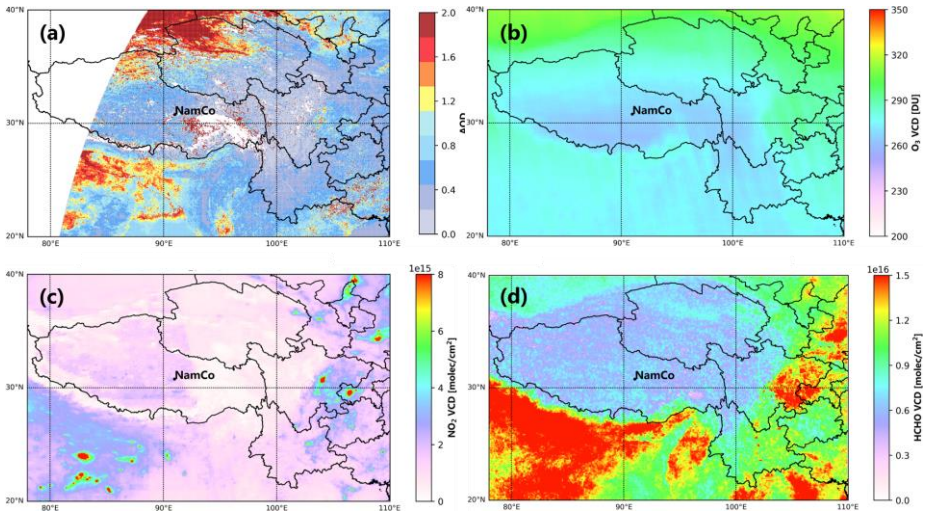

Figure S1. Averaged spatial distributions of (a) AOD monitored by Himawari-8, (b) O_3 total VCDs monitored by OMI, (c) NO_2 VCDs monitored by TROPOMI, (and d) HCHO VCDs monitored by TROPOMI from May to July 2019.

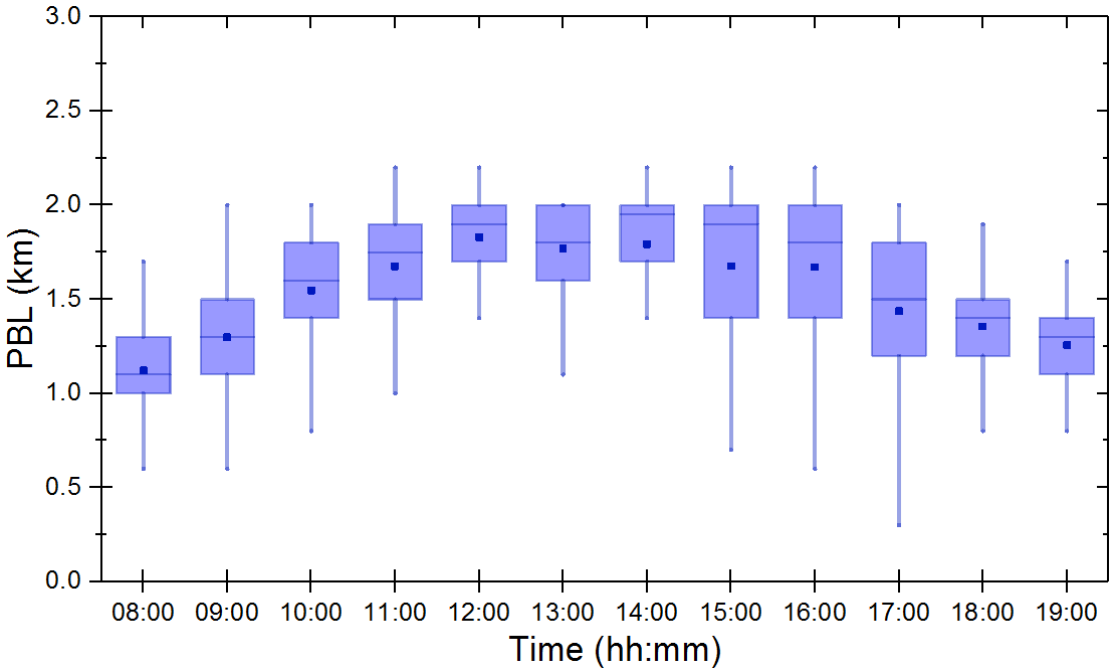

Figure S2. The diurnal variation of PBL in Nam Co from May to July 2019. The top and bottom of the box represented 75th and 25th percentiles, respectively. The lines and dots within the boxes were the median and mean, respectively.

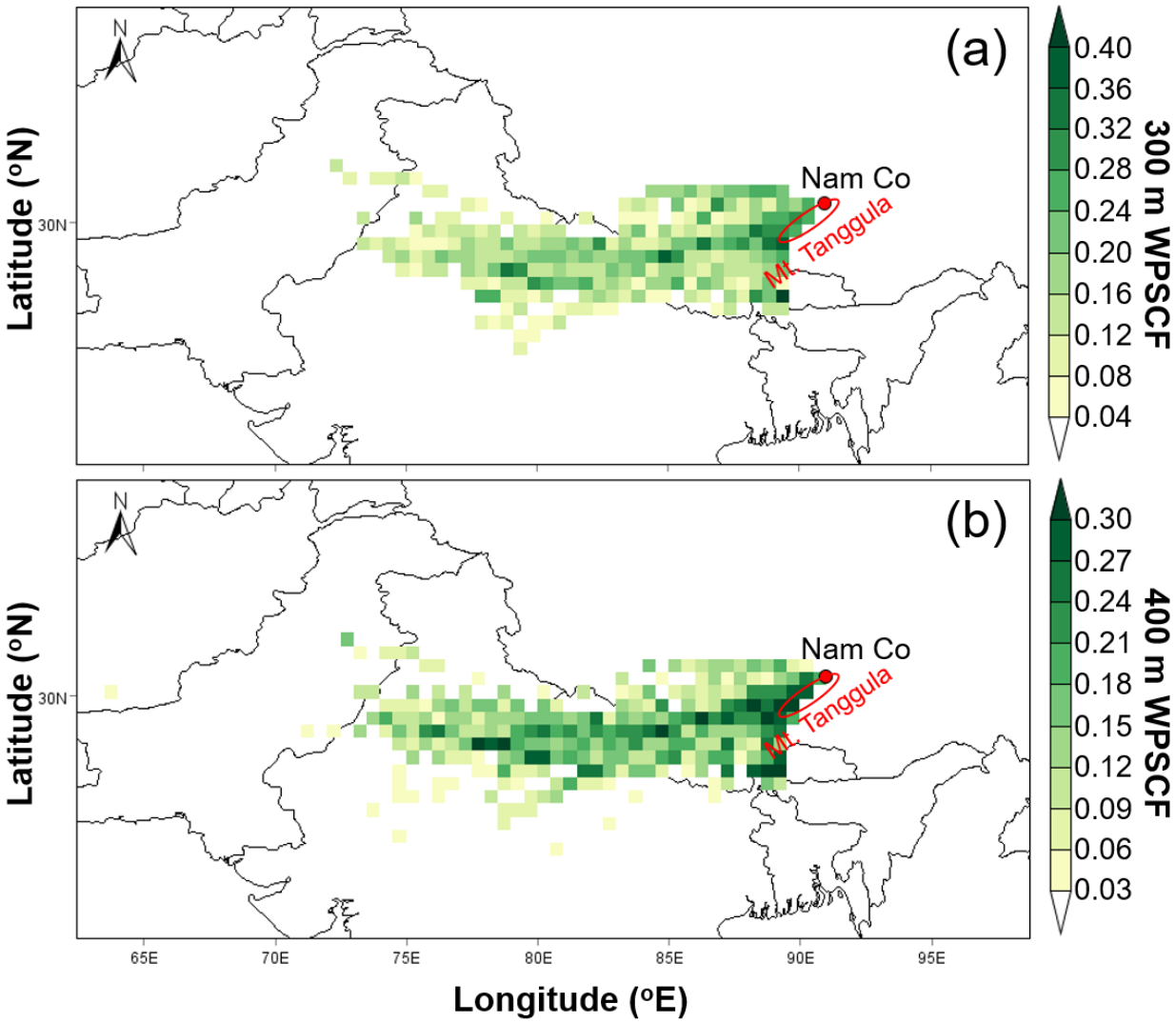

Figure S3. Spatial distributions of 24-h WPSCF values for NO_2 at (a) 300 m, and (b) 400 m height layers from 01 May to 09 July 2019 over CAS (NAMORS).

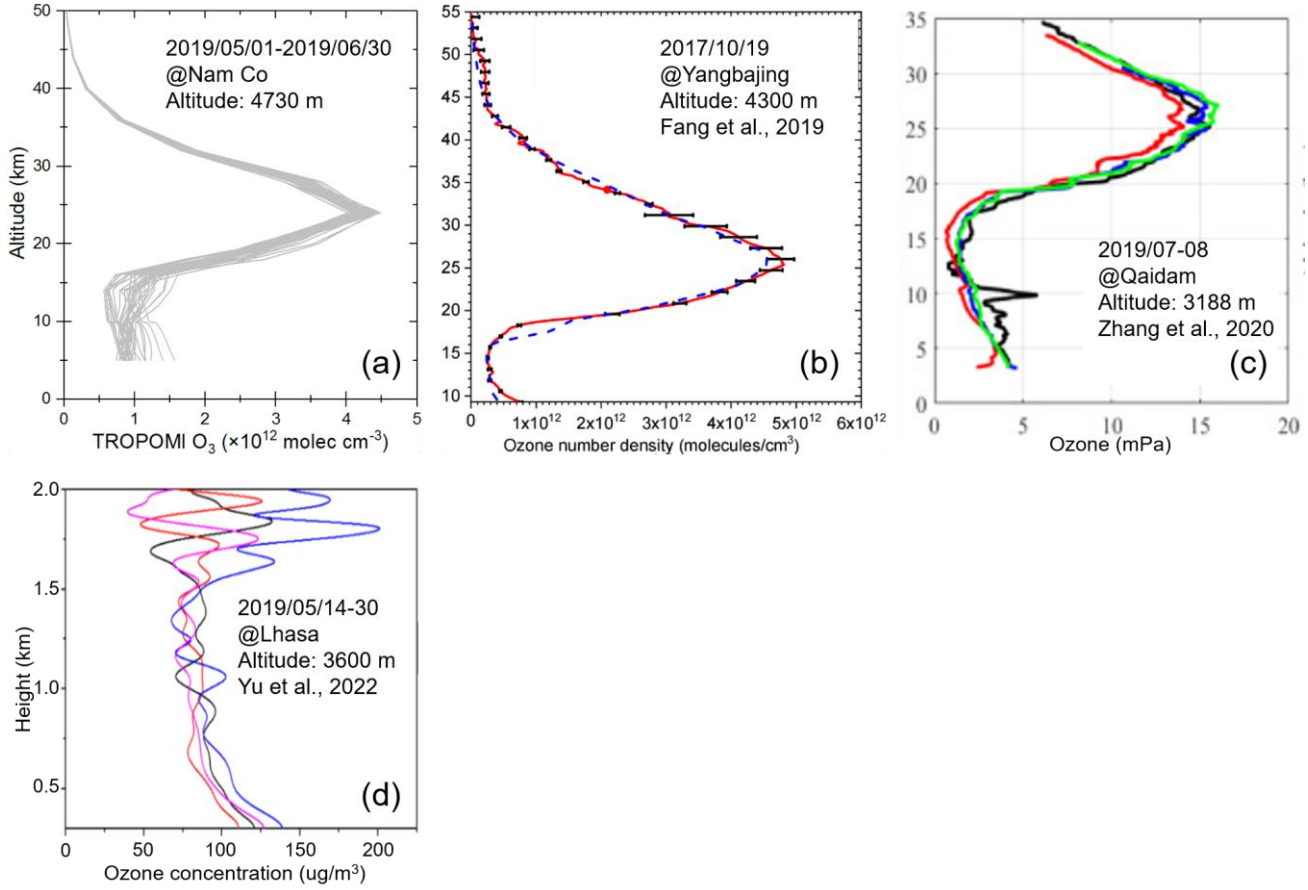

Figure S4. Ozone vertical profile measure by (a) TROPOMI at Nam Co, (b) lidar at Yangbajing (Feng et al., 2019), (c) ozonesonde at Qaidam (Zhang et al., 2020), and (d) lidar at Lhasa (Yu et al., 2022).

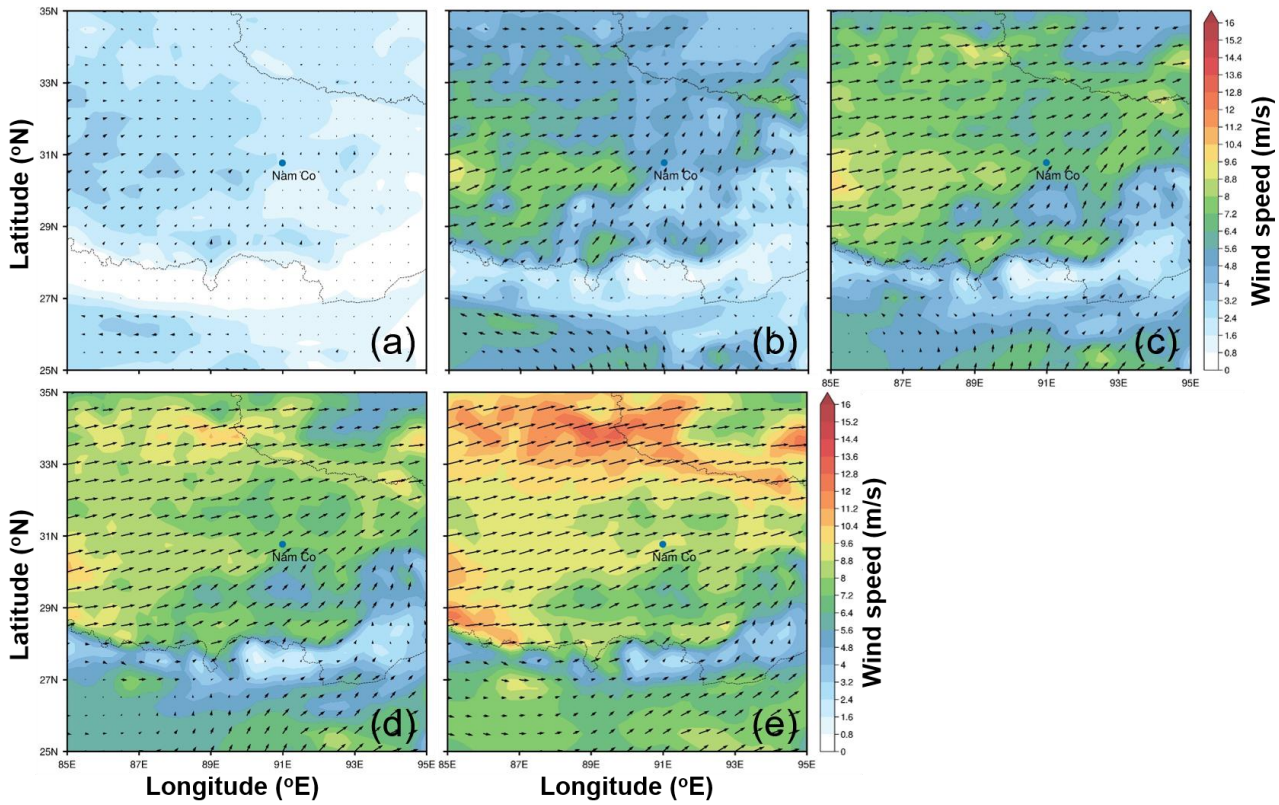

Figure S5. Wind direction and wind speed at (a) 10 m, (b) 500 m, (c) 1000 m, (d) 1300 m, and (e) 1800 m at a range of 25°N-35°N and 85°E-95°E, respectively.

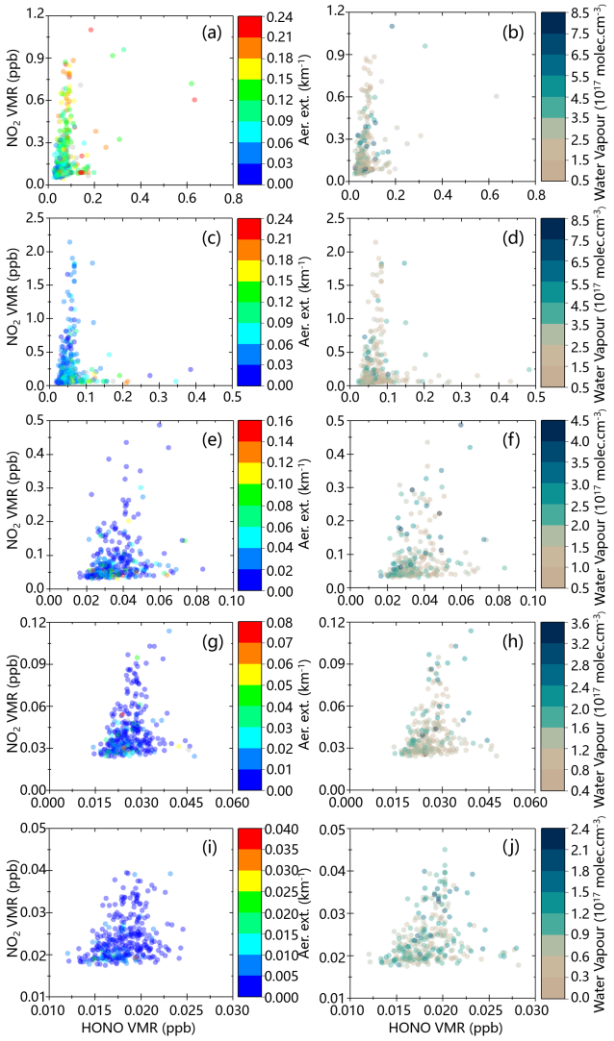

Figure S6. Scatter plots of HONO vs NO_2 at (a-b) 0-0.2 km, (c-d) 0.4-0.6 km, (e-f) 0.8-1.0 km, (g-h) 1.2-1.4 km, and (i-j) 1.6-1.8 km coloured by aerosol extinction coefficients and water vapour in the top and bottom row, respectively, from 01 May to 09 July 2019.

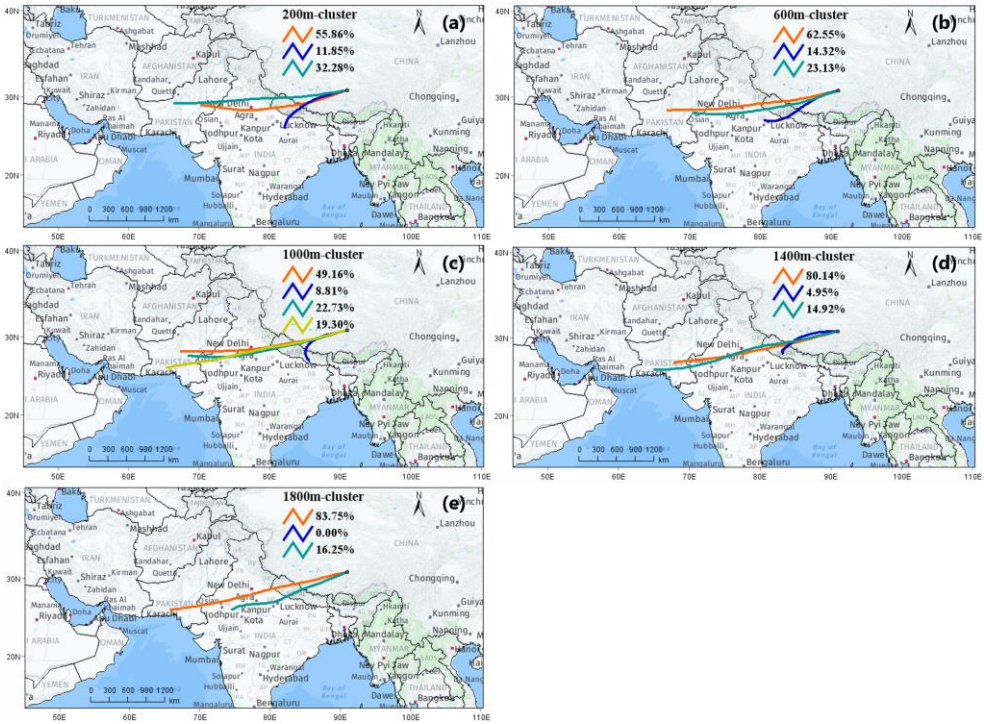

Figure S7. The percentage of allocation to each mean 48-h backward trajectory cluster arriving at CAS (NAMORS) at (a) 200 m, (b) 600 m, (c) 1000 m, (d) 1400 m, and (e) 1800 m height layers from 01 May to 09 July 2019.

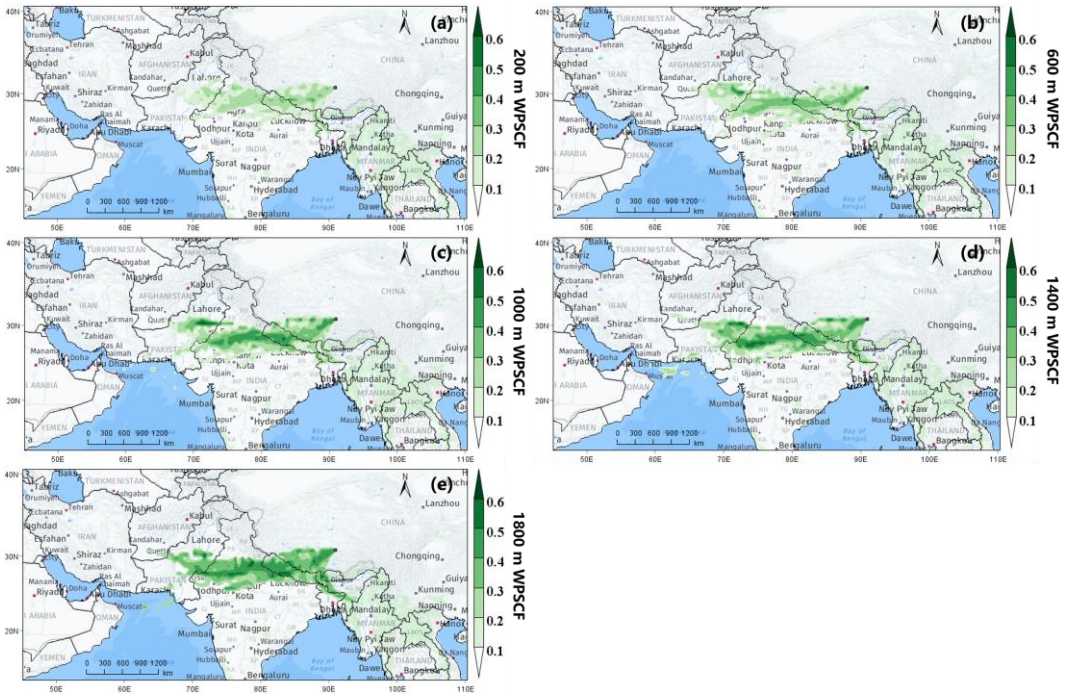

Figure S8. Spatial distributions of 48-h WPSCF values for O_3 at (a) 200 m, (b) 600 m, (c) 1000 m, (d) 1400 m, and (e) 1800 m height layers from 01 May to 09 July 2019 over CAS (NAMORS).

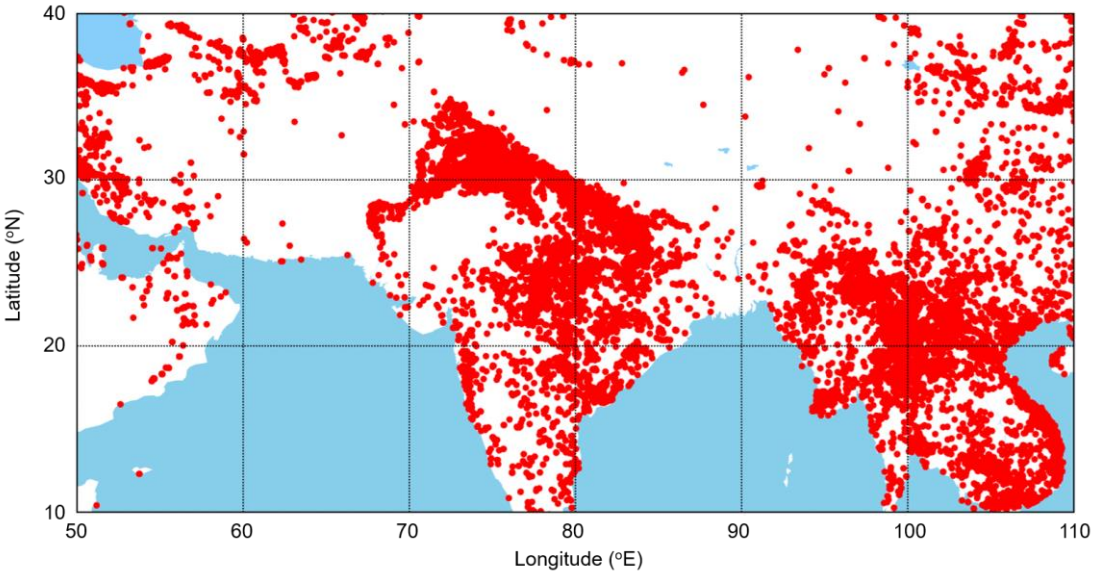

Figure S9. The spatial distribution of fire point in south Asian subcontinent from May to July 2019.

Appendix: WRF model configurations

The Weather Research and Forecasting (WRF) model was used to simulate the planetary boundary layer (PBL) height on the Tibetan Plateau. The detailed description of WRF model was given in the WRF website (http://www.wrf-model.org/index.php). In this work, the simulation domain covered 25°N-35°N and 80°E-100°E. The horizontal resolution of this simulation was set to 20×20 km^2, and we set 26 hybrid pressure-sigma levels in the vertical direction. We selected the 6-h final operational global analysis (FNL) data as the initial meteorological fields and boundary conditions. The data were provided by the National Centers for Environmental Prediction (NCEP) with a $1^o \times 1^o$ spatial resolution. Moreover, the NCEP Administrative Data Processing (ADP) Global Surface Observational Weather Data (ds461.0) and Upper Air Observational Weather Data (ds351.0) with 6-h temporal resolution were used to accurately reproduce the methodology. The physical parameterization schemes adopted in this study were described in Table S1.

Table S1. Model physical parameterization schemes.

Schemes	Description
Microphysics	Purdue Lin Scheme (Chen et al., 2002)
Longwave radiation	Rapid radiative RRTMG Scheme (Iacono et al., 2008)
Shortwave radiation	RRTMG Scheme (Iacono et al., 2008)
Cumulus parameterization	Grell-Freitas Ensemble Scheme (Grell et al., 2014)
Land surface	Unified Noah Land Surface Model (Tewari et al., 2004)
Planetary boundary layer	Yonsei University Scheme (Hong et al., 2006)

References

[1] Fang, X., Li, T., Ban, C., Wu, Z., Li, J., Li, F., Cen, Y., and Tian, B.: A mobile differential absorption lidar for simultaneous observations of tropospheric and stratospheric ozone over Tibet, Opt. Express, 2019, 27(4), 4126-4139, doi:10.1364/OE.27.004126.

[2] Yu, J., Meng, L., Chen, Y., Zhang, H., and Liu, J.: Ozone profiles, precursors, and vertical distribution in urban Lhasa, Tibetan Plateau, Remote Sens., 2022, 14(11), doi:10.3390/rs14112533.

[3] Zhang, J., Xia, X., and Wu, X.: First in situ UV profile across the UTLS accompanied by ozone measurement over the Tibetan Plateau, J. Environ. Sci., 2020, 98, 71-76, doi:10.1016/j.jes.2020.05.020.